Available online at www.sciencedirect.com
ScienceDirect
Journal of Photochemistry and Photobiology A: Chemistry 187 (2007) 78–86
Journal of Photochemistry and Photobiology A:Chemistry
www.elsevier.com/locate/jphotochem

Photophysical properties of some donor–acceptor 1*H*-pyrazolo[3,4-*b*]quinolines Radiative versus non-radiative electron transfer processes

Marek Mac [a,*], Tomasz Uchacz [a], Marcin Andrzejak [a], Andrzej Danel [b], Paweł Szlachcic [b]

[a] *Faculty of Chemistry, Jagiellonian University, Ingardena St. 3, 30-060 Kraków, Poland*
[b] *Departament of Chemistry, University of Agriculture, Balicka St. 122, 31-149 Kraków, Poland*

Received 24 July 2006; received in revised form 19 September 2006; accepted 5 October 2006
Available online 12 October 2006

Abstract

The fluorescence behaviour of some new dyes based on the pyrazolo[3,4-*b*]quinoline (PQ) ring has been investigated. It was found that introduction of electron withdrawing and electron donating groups into pyrazolo[3,4-*b*]quinoline molecule causes an increase of the ground and excited state dipole moments but more important is introduction of the *N*,*N*-dimethylamine group directly into the pyrazolo[3,4-*b*]quinoline skeleton. Further introduction of the cyano groups in the peripheral phenyl rings brings about only minor changes in the transition dipole moments (absorption and fluorescence). Such compounds exhibit a CT fluorescence. The fluorescence of these compounds was investigated in terms of the radiative charge transfer transition to obtain the charge transfer parameters such as the energy gap between the charge transfer and the ground states, solvent reorganization energies and internal reorganization energy. The magnitude of these parameters was discussed in terms of a modern electron transfer theory and the parameters were used to calculate the rate constants for non-radiative CT transition.

Keywords: CT fluorescence; Electron transfer; Radiative transition; Non-radiative transition

1. Introduction

Since the first synthesis of pyrazolo[3,4-*b*]quinoline (PQ) by Musierowicz et al. [1] in 1928 that class of compounds was of interest as possible antiviral agents inducing the formation of interferon [2], antiviral properties [3] and potential antimalarials [4]. Several members of this ring system fluorescence and have been proposed as optical brighteners for acetate and polyester fibres [5].

The pyrazoloquinolines are highly emissive in solvents [6] as well as in the solid state. Owing to their emissive properties they are good candidates for construction of brightly fluorescent molecular sensors [7] and luminescent materials for fabrication of organic light emitting diodes (OLED) [8]. We applied some pyrazoloquinolines for this purpose as dopants in PVK matrices [9], vacuum deposited films [10] and polymers [11]. In addition, some pyrazolo[3,4-*b*]quinolines with nitro and *N*,*N*-dimehylamino substituents appear to be good building blocks for non-linear optical materials [12,13].

Following our line of investigation presented in the previous paper [14], where we reported on the photophysical investigation of some heterocyclic dyes containing the pyrazoloquinoxaline (PQX) skeleton [14], we found that introduction of the dimethylamine group greatly enhances the charge transfer character of the luminescence of the dye. This effect manifests itself by the strong solvent polarity dependence of the fluorescence parameters such as lifetimes, quantum yields and the position of the fluorescence maximum. The fluorescence studies were accompanied by the transient absorption measurements, which showed the correspondence of the fluorescence efficiency and lifetimes with the relative efficiency of the population of the lowest triplet state, and their mutual dependence on the solvent polarity. The experimental data let us to believe that in pyrazoloquinoxalines the lowest triplet state is populated via $S_1 \Rightarrow T_n \Rightarrow T_1$ sequential mechanism, the efficiency of which is governed by the S_1–T_n energy gap.

* Corresponding author. Tel.: +48 12 6632262; fax: +48 12 6340515.
E-mail address: mac@chemia.uj.edu.pl (M. Mac).

1010-6030/$ – see front matter © 2006 Elsevier B.V. All rights reserved.
doi:10.1016/j.jphotochem.2006.10.001

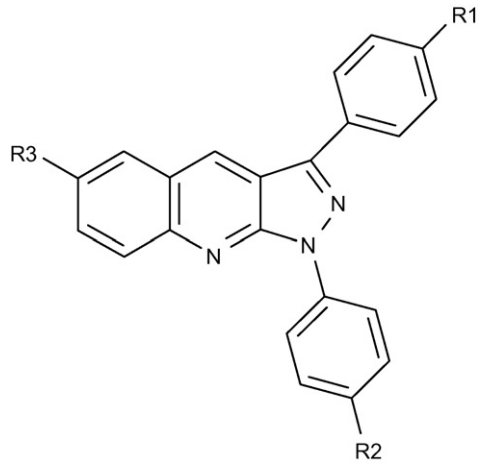

Fig. 1. Chemical structures of the investigated pyrazoloquinolines (PQ): R1 = R2 = R3 = H 1,3-diphenyl-1*H*-pyrazolo[3,4-*b*]quinoline (PQ1); R1 = R2 = H R3 = $N(CH_3)_2$ 6-dimethylamino-1,3-diphenyl-1*H*-pyrazolo[3,4-*b*]quinoline (PQ2); R1 = CN R2 = H R3 = $N(CH_3)_2$ 3-(4-cyanophenyl)-6-dimethylamino-1-phenyl-1*H*-pyrazolo[3,4-*b*]quinoline (PQ3); R1 = H R2 = CN R3 = $N(CH_3)_2$ 1-(4-cyanophenyl)-6-dimethylamino-1-phenyl-1*H*-pyrazolo[3,4-*b*]quinoline (PQ4).

In this paper we examine fluorescence behaviour of pyrazoloquinolines—another class of efficiently fluorescing and photochemically stable heterocyclic compounds (see Fig. 1).

2. Experimental

2.1. Synthesis of 1H-pyrazolo[3,4-b]quinolines

2.1.1. The synthesis of pyrazolones and pyrazolocarbaldehydes-general procedures

Pyrazolones **1a**,**1b** were prepared on 1 h refluxing equimolar amounts (0.02 mol) of appropriate phenylhydrazine and β-ketoester in ethanol (50 mL). Half of the solvent was removed *in vacuo*. After cooling the resulting precipitate was filtered off and recrystallized from the 4:1 ethanol/water mixture.

*2.1.1.1. 2-(4-Bromophenyl)-5-phenyl-2,4-dihydropyrazolin-3-one (**1a**).* Yellow crystals, mp 151–152 °C, 57% yield. Anal. Calcd. for $C_{15}H_{11}BrN_2O$: C, 57.16; H, 3.52; N, 8.89. Found: C, 56.98; H, 3.49; N, 8.76.

*2.1.1.2. 5-(4-Bromophenyl)-5-phenyl-2,4-dihydropyrazolin-3-one (**1b**).* Light yellow crystals, mp 169–170 °C, 77% yield. Anal. Calcd. for $C_{15}H_{11}BrN_2O$: C, 57.16; H, 3.52; N, 8.89. Found: C, 56.87; H, 3.39; N, 8.61.

Phosphorous oxychloride (0.07 mol, 6.4 mL) was added dropwise to ice cooled DMF (0.03 mol, 2.3 mL). On agitation, a pyrazolin-3-one (0.01 mol) was added dropwise within 15 min to that Vilsmeier-Haack reagent maintaining room temperature followed by 1 h heating at 110 °C. After cooling, the reaction mixture was poured to 100 mL ice/water. Precipitated crystals were filtered, washed with water, dried, and recrystallized from ethanol.

*2.1.1.3. 1-(4-Bromophenyl)-5-chloro-3-phenyl-1H-pyrazolo-4-carbaldehyde (**2a**).* White crystals, mp 140–142 °C, 71% yield. ^{1}H NMR ($CDCl_3$, 300 MHz, δ ppm): 10.06 (s, 1H, CHO); 7.81–7.78 (m, 2H); 7.69 (d, J = 8.8 Hz, 2H); 7.54 (d, J = 8.8 Hz, 2H); 7.52–7.47 (m, 3H). Anal. Calcd. for $C_{16}H_{10}BrClN_2O$: C, 53.14; H, 2.79; N, 7.74. Found: C, 53.04; H, 2.64; N 7.65.

*2.1.1.4. 3-(4-Bromophenyl)-5-chloro-1-phenyl-1H-pyrazolo-4-carbaldehyde (**2b**).* White crystals, mp 178–179 °C, 67% yield. ^{1}H NMR (300 MHz, $CDCl_3$, δ ppm): 10.05 (s, 1H, CHO); 7.80, 7.79 (d, J = 8.6 Hz, 2H); 7.63–7.54 (m, 7H). Anal. Calcd. for $C_{16}H_{10}BrClN_2O$: C, 53.14; H, 2.79; N, 7.74. Found: C, 52.95; H, 2.58; N 7.63.

2.1.1.5. 1-H-Pyrazolo[3,4-b]quinolines: general procedure. *N*,*N*-Dimethyl-1,4-phenylenediamine (0.01 mol, 1.3 g) and either **2a** or **2b** (0.01 mol, 3.6 g) were heated slowly for 20 min on an oil bath at 140–200 °C. After cooling, the melt was boiled with ethanol (50 mL) and filtered. The crude product was dissolved in $CHCl_3$ (50 mL) and subjected to a column chromatography on aluminium oxide (Merck, neutral, II-III Brockmann). The chromatography procedure was repeated on a column packed with silica-gel (Merck 60, 70–230 mesh) and developed with the toluene/ethyl acetate (3:1).

*2.1.1.6. 1-(p-Bromophenyl)-6-N,N-dimethylamine-3-phenyl-1H-pyrazolo[3,4-b]quinoline (**3a**).* Yellow crystals, mp 155–156 °C (toluene), 55% yield. ^{1}H NMR (300 MHz, $CDCl_3$, δ ppm): 8.71 (s, 1H, 4-H); 8.56 (d, J = 8.9 Hz, 2H, 2,6-H_{1Ph}); 8.14 (d, J = 7.06, 2H); 8.05 (d, J = 9.5 Hz, 1H); 7.66 (d, J = 8.9 Hz, 2H, 3,5-H_{1Ph}); 7.61–7.56 (m, 3H); 7.49 (t, J = 7.3 Hz, 1H); 3.11 (s, 6H, Me_2N–). Anal. Calcd. for $C_{24}H_{19}BrN_4$: C, 65.02; H, 4.31; N, 12.63. Found: C, 64.89; H, 4.16; N 12.49.

*2.1.1.7. 3-(p-Bromophenyl)-6-N,N-dimethylamine-1-phenyl-1H-pyrazolo[3,4-b]quinoline (**3b**).* Yellow crystals, mp 183–184 °C (toluene), 60% yield. ^{1}H NMR (300 MHz, $CDCl_3$, δ ppm): 8.66 (s, 1H, 4-H); 8.58(d, J = 8.1 Hz, 2H, 2.6-H_{1Ph}); 8.08–8.03 (m, 3H); 7.70(d, J = 8.5 Hz, 2H); 7.58–7.54 (m, 3H, 3,5-H_{1Ph}); 7.26 (t, J = 7.4Hz, 1H, 4-H_{1Ph}); 6.98 (d, J = 2.7 Hz, 1H, 5-H); 3.1 (s, 6H, Me_2N–). Anal. Calcd. for $C_{24}H_{19}BrN_4$: C, 65.02; H, 4.31; N, 12.63. Found: C, 64.75; H, 4.11; N 12.51.

A solution of either **3a** or **3b** (0.005 mol, 2.2 g) and CuCN (0.006 mol, 0.54 g) in 5 mL of *N*-methyl-2-pyrrolidinone (NMP) was heated at 150 °C for 5 h. The reaction mixture was cooled and poured into water (20 mL). The precipitate was filtered off, dried, dissolved in a minimum amount of $CHCl_3$ and filtered off to remove inorganic residues. The solution was subjected to a column chromatography on silica gel (Merck 60, 70–230 mesh) using $CHCl_3$ as eluent (Fig. 2).

*2.1.1.8. 1-(p-Cyanophenyl)-6-dimethylamino-3-phenyl-1H-pyrazolo[3,4-b]quinoline (**4a**-PQ4).* Yellow crystals, mp 242–243 °C (toluene), 55% yield. ^{1}H NMR ($CDCl_3$, 300 MHz, δ ppm): 8.88 (d, J = 8.5 Hz, 2H, 2,6-H_{1Ph}); 8.63 (s, 1H, 4-H); 8.11 (d, J = 7.4 Hz, 2H, 2,6-$H_{3\text{-}Ph}$); 8.02 (d, J = 9.6 Hz, 1H,

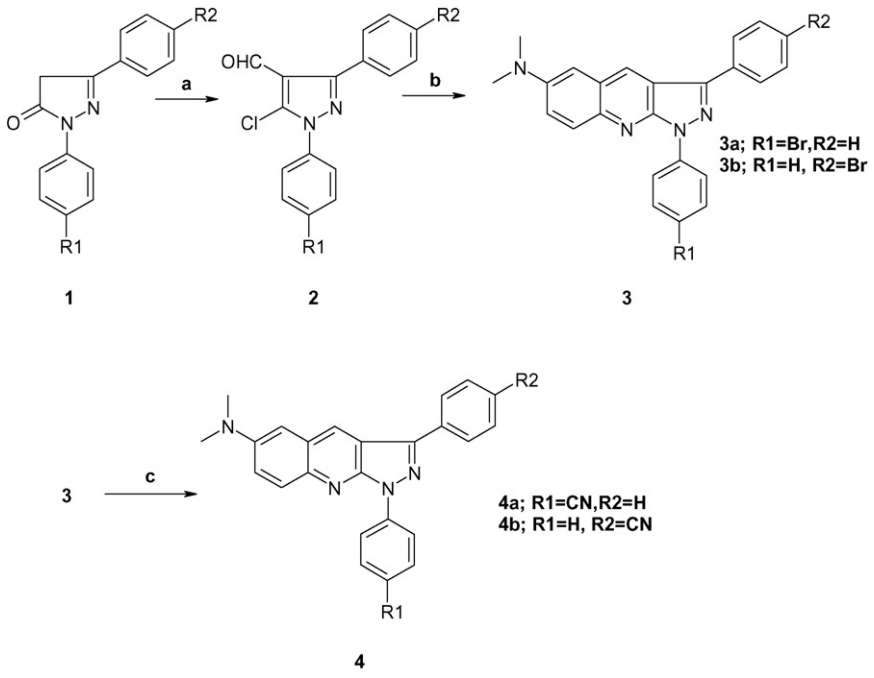

Fig. 2. (a) $POCl_3$/DMF/110 °C; (b) *N*,*N*-dimethyl-1,4-phenylenediamine/140–180 °C; (c) CuCN/*N*-methyl-2-pyrrolidinone/180–190 °C.

8-H); 7.80 (d, $J = 8.5$ Hz, 3,5-$H_{1\text{-Ph}}$); 7.62–7.48 (m, 4H); 6.92 (d, $J = 2.4$ Hz, 1H, 5-H); 3.09 (s, 6H, Me_2N–). Anal. Calcd. for $C_{25}H_{19}N_5$: C, 77.09; H, 4.91; N, 17.97. Found: C, 76.96; H, 4.87; N 17.79.

*2.1.1.9. 3-(p-Cyanophenyl)-6-dimethylamino-1-phenyl-1H-pyrazolo[3,4-b]quinoline (**4b**-PQ3).* Red crystals, mp 238–240 °C (toluene), yield 61%. ^{1}H NMR ($CDCl_3$, 300 MHz, δ ppm): 8.66 (s, 1H, 4-H); 8.56 (d, $J = 8.2$ Hz, 2H, 2,6-$H_{1\text{-Ph}}$); 8.28 (d, $J = 8.2$ Hz, 2H); 8.06 (d, $J = 9.6$Hz, 1H, 8-H); 7.83 (d, $J = 8.2$ Hz, 2H); 7.60–7.55 (m, 3H); 7.32 (t, $J = 7.4$ Hz, 1H, 4-$H_{1\text{-Ph}}$); 6.97 (d, $J = 2.2$ Hz, 1H, 5-H); 3.11 (s, 6H, Me_2N–). Anal. Calcd. for $C_{25}H_{19}N_5$: C, 77.09; H, 4.91; N, 17.97. Found: C, 76.88; H, 4.76; N, 17.81.

2.1.1.10. 1,3-Diphenyl-1H-pyrazolo[3,4-b]quinoline (PQ1). It was prepared by the Friedländer condensation of *o*-aminobenzaldehyde with 2,5-diphenyl-2,4-dihydropyrazol-3-one [15].

2.1.1.11. 6-Dimethylamino-1,3-diphenyl-1H-pyrazolo[3,4-b]quinoline (PQ2). Equimolar amounts of *N*,*N*-dimethyl-*p*-phenylenediamine (0.013 mol) and 1,3-diphenyl-5-chloro-4-formylpyrazole (0.01 mol) were heated in sulfolane (5 mL) at 140–190 °C for 20 min. After cooling, the reaction mixture was poured into water and filtered off. The solid was dried, dissolved in $CHCl_3$ passed by alumina (Merck, neutral, II–III Brockmann). Finally it was chromatographed (3 times) on silica gel (Merck 60, 70–230 mesh).

Yellow crystals, mp 200–201 °C, 35% yield. ^{1}H NMR ($CDCl_3$, 300 MHz, δ ppm): 8.73 (s, 1H, 4-H); 8.61 (d, $J = 8.1$ Hz, 2H, 2,6-H_{1Ph}); 8.16 (d, $J = 7.4$ Hz, 2H, 2,6-H_{3Ph}); 8.07 (d, $J = 9.5$ Hz, 1H, 8-H); 7.61–7.46 (m, 6H); 7.48 (t, $J = 7.3$ Hz, 1H); 7.29 (t, $J = 7.4$ Hz, 1H); 3.11 (s, 6H, Me_2N). Anal. Calcd. for $C_{24}H_{20}N_4$: C, 79.10; H 5.53; N, 15.37. Found: C, 78.99; H, 5.44; N, 15.21.

2.1.2. Fluorescence measurements (steady state and time-resolved)

The solvents: cyclohexane (CHX), dibutyl ether (DBE), ethyl acetate (EtAc), tetrahydrofuran (THF), ethyl bromide (EtBr), ethyl iodide (EtI), glycerol triacetate (GTA), dichloromethane ($MeCl_2$), propanol (PrOH), acetone (ACE), methanol (MeOH), acetonitrile (ACN), dimethylformamide (DMF), propylene carbonate (PC) and dimethyl sulfoxide (DMSO) were of spectroscopic grade and were used as received (all from Aldrich). All the solvents did not show any traces of fluorescence. For fluorescence and transient absorption measurements the solutions of the dyes were degassed using the freeze-pump-thaw cycles. The sample concentration of the dyes for spectroscopic measurements is ca. 10^{-5} M (it refers to absorbances of ca. 0.2–0.3 at excitation wavelength in the fluorescence investigations).

Fluorescence measurements were performed on a home-built spectrofluorimeter and a time-correlated single photon counting arrangement [14]. For time-resolved fluorescence measurements a picosecond diode laser ($\lambda = 400$ nm, 70 ps pulse duration) or a nanosecond diode ($\lambda = 370$ nm, 1 ns pulse duration) (both from IBH-UK) as excitation source were used. For steady-state fluorescence measurements a 365 or 405 nm line of medium-pressure mercury lamp was used. The fluorescence quantum yields measurements were carried out with quinine sulphate in water ($\Phi_{fl} = 0.55$) [16] as an actinometer.

2.1.3. Calculations

Electron transfer parameters were recovered using the CT fluorescence band shape analysis, described in previous papers

[14,17]. For minimization the MINUITS procedure from the CERN Library was employed.

3. Results

3.1. Absorption and fluorescence measurements

Absorption and fluorescence spectra of pyrazoloquinolines (PQ) in ethyl bromide are presented in Figs. 3 and 4.

Absorption of pyrazoloquinolines shifts bathochromically when the electrodonating group (dimethylamine) is introduced in the 6-position of the pyrazoloquinoline skeleton (ca. 3000 cm^{-1}). Introduction of the cyano group in the *para* position of the peripheral phenyl rings (located either in position 1 or 3) brings about only a small change of the position of the lowest absorption band. The same is valid for the fluorescence spectra: again, the strong bathochromic shift is observed upon substitution of the hydrogen atom by the amino group and subsequent introduction of the cyano groups does not affect so significantly the position of the fluorescence maximum (ca. 400–800 cm^{-1})

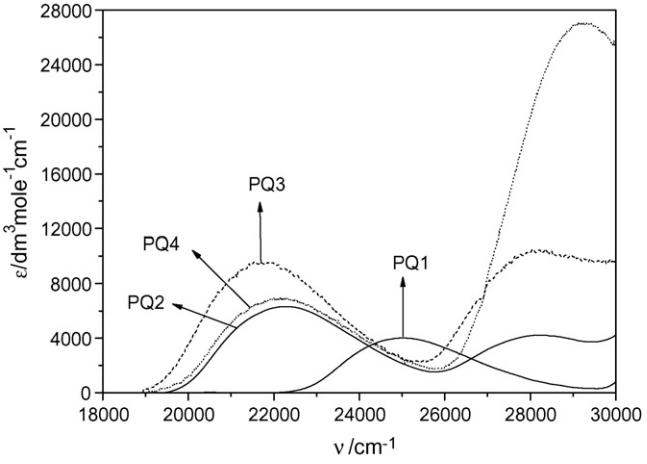

Fig. 3. Absorption spectra of pyrazoloquinolines (PQ1–PQ4) in ethyl bromide.

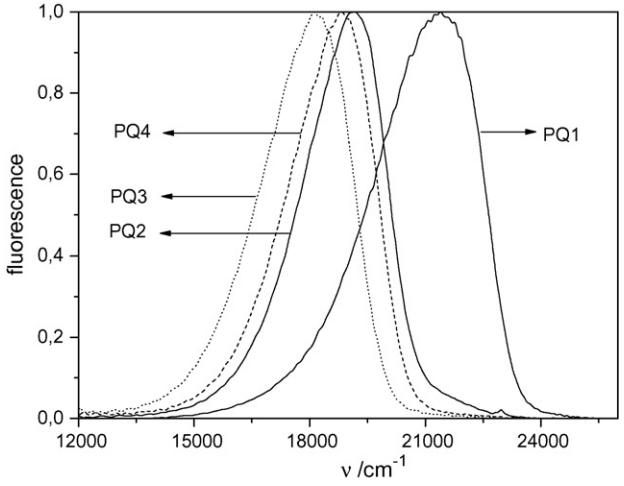

Fig. 4. Fluorescence spectra of pyrazoloquinolines (PQ1–PQ4) in ethyl bromide normalised and corrected for spectral sensitivity of the detector.

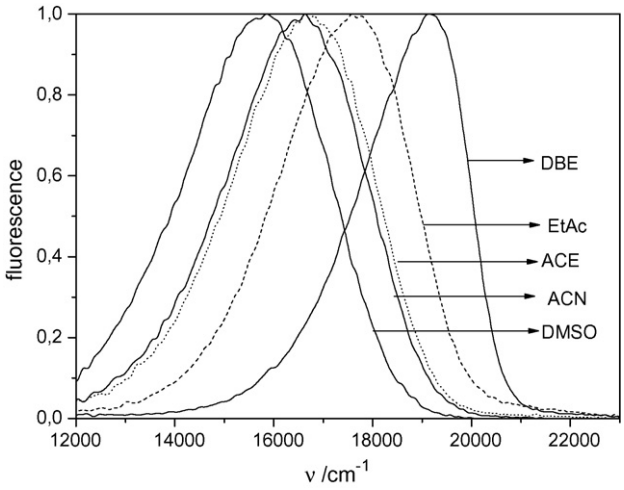

Fig. 5. Fluorescence spectra of compound PQ3 in solvents of different polarity (as indicated by the acronyms in the figure), DBE: dibutyl ether ($\varepsilon_s = 3.08$); EtAc: ethyl acetate ($\varepsilon_s = 6.08$); ACE: acetone ($\varepsilon_s = 21.0$); ACN: acetonitrile ($\varepsilon_s = 36.6$); DMSO: dimethylsulfoxide ($\varepsilon_s = 47.2$).

as the introduction of the amine group to the parent molecule PQ1 (ca. 2000–3000 cm^{-1}).

Fluorescence spectra of PQ1 are relatively weakly dependent on the solvent polarity, and in non-polar cyclohexane a small vibrational structure is observed in the spectrum. Appearance of a dimethylamine group introduced to the pyrazoloquinoline skeleton of PQ1 causes a significant solvatochromic shift in fluorescence spectr a, further amplified by introduction of the cyano groups attached in the *para* position to the peripheral phenyl rings. This may indicate that the excited state dipole moment increases upon introduction of the cyano groups into the PQ2 molecule. We observe a considerable batochromic shift in the position of the fluorescence maximum as indicated in Fig. 5, which can be accounted for by assuming that the emitting singlet state has a dipole moment much larger than the ground state, strongly suggesting that it has an internal charge transfer character. For such a biradical-type state the dipole-moment can be experimentally calculated from the Lippert–Mataga relationship, neglecting a mean solute polarizability ($\alpha \approx \alpha_e \approx \alpha_g \approx 0$) [18].

The photophysical properties of the investigated pyrazoloquinolines in several solvents of different polarity are presented in Table 1.

The position of the maxima of the absorption band for the compounds PQ2, PQ3 and PQ4 depends on solvent polarity only slightly, contrary to that of the emission as shown in Fig. 5. If the CT fluorescence originates from the state reached directly by excitation, the excited state dipole moment can be calculated from the solvatochromic shifts of the absorption and fluorescence spectra. Mathematically, this dependence is described by the well-known Lippert–Mataga equation [18]

$$\nu_{abs} - \nu_{flu} = \frac{\Delta\vec{\mu}^2}{2\pi\varepsilon_0 hca^3}\left(\frac{\varepsilon_s - 1}{2\varepsilon_s + 1} - \frac{n^2 - 1}{2n^2 + 1}\right), \quad (1)$$

where ν_{abs} and ν_{flu} are the spectral positions of the maximum of the CT absorption and equilibrated emission bands, respectively,

Table 1
Absorption and fluorescence parameters of compounds PQ1–PQ4 in solvents of different polarities

Solvent	Quantum yield	Fluorescence lifetime (ns)	ν^{a}_{max}	ν^{f}_{max} (ν_{av})	M_a/D	M_f/D
PQ1						
CHX	0.86	17.9	24910	22540 (21369)	2.02	2.22
DBE	0.88	18.6	25090	21980 (21000)	2.03	2.18
EtBr	0.5	18.5	25090	21390 (20732)	1.98	2.12
GTA	0.87	20.8	25090	21200 (20390)	2.24	2.33
MeOH	0.71	25.5	25210	21080 (20492)	2.06	2.1
CAN	0.73	25.1	25200	20920 (20341)	1.94	2.0
PQ2						
CHX	0.84	16.1	22750	(19917)	3.00	2.84
DBE	0.77	18.4	22490	20050 (19384)	3.01	2.74
EtAc	0.60	21.5	22390	18780 (18323)	2.72	2.5
THF	0.84	21.0	22220	18720 (18205)	3.0	2.92
EtBr	0.65	16.3	22220	19140 (18700)	2.72	2.75
EtI	0.24	7.2	22220	19160	2.71	
$MeCl_2$	0.75	19.9	22160	18880 (18054)	3.0	2.82
ACE	0.58	23.4	22200	18090 (17700)	2.85	2.53
MeOH	0.52	22.5	22330	17380 (17077)	3.08	2.66
ACN	0.57	24.5	22260	17810 (17490)	2.86	2.53
PC	0.56	23.0	22040	17650 (17262)	2.85	2.43
PQ3						
CHX	0.72	11.2	22260	20170	3.27	
DBE	0.79	14.0	22090	19170 (18522)	3.1	3.20
EtAc	0.65	14.8	22000	17680 (17259)	3.22	3.25
THF	0.69	15.3	21740	17570 (17087)	3.21	3.20
EtBr	0.60	13.8	21770	18200 (17618)	3.20	2.94
EtI	0.23	6.2	21570	18370 (17659)	2.84	2.50
$MeCl_2$	0.69	16.2	21770	18020 (17453)	3.25	2.97
ACE	0.58	17.1	21770	16770 (16395)	3.15	3.14
MeOH	0.34	11.4	21970	16350 (16043)	3.20	3.15
ACN	0.47	17.5	21900	16610 (16235)	3.15	3.40
PC	0.37	14.0	21670	16280 (15900)	3.22	3.05
DMSO	0.23	11.0	21470	15810 (15500)		2.95
PQ4						
CHX	0.64	15.1	22580	20580		
DBE	0.68	19.4	22420	19620 (18552)	2.75	2.67
EtAc	0.75	23.9	22270	18300 (17736)	2.45	2.78
THF	0.65	23.1	22250	18240 (17663)	2.75	2.56
EtBr	0.64	18.0	22180	18840 (18225)	2.73	2.7
EtI	0.24	7.0	21910	18880	2.78	2.41
$MeCl_2$	0.63	21.5	22140	18630 (18018)	2.74	2.48
PrOH	0.54	20.1		17760 (17340)		2.63
ACE	0.58	25.3	22240	17600 (17100)	2.65	2.56
MeOH	0.38	21.2	22260	17170 (16850)	2.74	2.39
ACN	0.62	26.0	22320	17430 (16960)	2.67	2.57
PC	0.53	23.0	22110	16930 (16460)	2.56	2.53
DMSO	0.46	19.9	21930	16480 (16036)	2.30	2.46

The parameters have the following meanings: ν^{a}_{max}, position of the longwave absorption maximum; ν^{f}_{max}, position of the fluorescence maximum; ν_{av}, averaged emission frequency; M_a and M_f denote the transition dipole moments for absorption and emission, respectively. For the calculation of the last three parameters see the following part of the text.

$\Delta\vec{\mu} = \vec{\mu}_e - \vec{\mu}_g$ is the difference between the excited and ground state dipole moments, respectively, ε_0 the dielectric permittivity of the vacuum, and a is the radius of the Onsager cavity. The parameters ε_s and n are the static dielectric constant and refraction index of the solvent (Fig. 6).

Similar behaviour has been found for PQ4, where the slope in the Lippert–Mataga dependency was 11590 (1100) cm^{-1}. The semiempirical calculations (HYPERCHEM, AM1 parametrization) yielded the ground-state dipole moments equal to 5.53 and 8.31D for PQ3 and PQ4, respectively. Assuming 5.9 Å (calculated from the molecular volume for PQ1—HYPERCHEM, AM1 parametrization) to be the effective radius of the Onsager cavity for both molecules, we obtain the values for dipole moments changes upon excitation equal to 14.85 (1.4) and 13.1 (1.3)D for PQ3 and PQ4, respectively. The similar procedure has been employed for PQ2. Again the ground state dipole moment

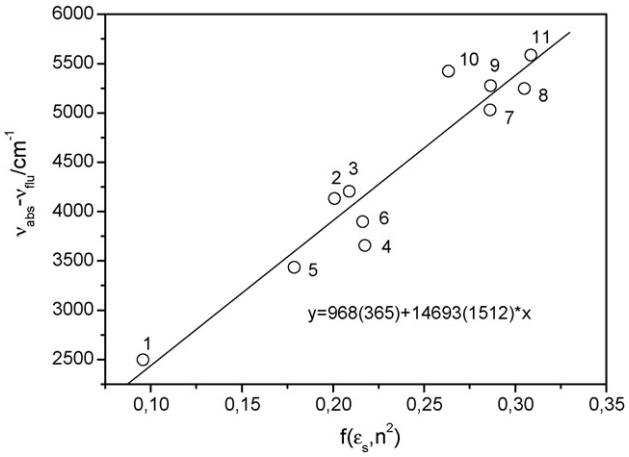

Fig. 6. Lippert–Mataga plot for the dependence of the difference between the position of the maxima of the absorption and fluorescence bands on solvent polarity function $f(\varepsilon_s, n^2) = (((\varepsilon_s - 1)/(2\varepsilon_s + 1)) - ((n^2 - 1)/(2n^2 + 1)))$ for PQ3 (correlation coefficient $R = 0.96$). The solvents (indicated by the numbers) are 1: DBE; 2: EtAC; 3: THF; 4: EtBr; 5: EtI; 6: $MeCl_2$; 7: ACE; 8: ACN; 9: PC; 10: DMSO; 11: MeOH.

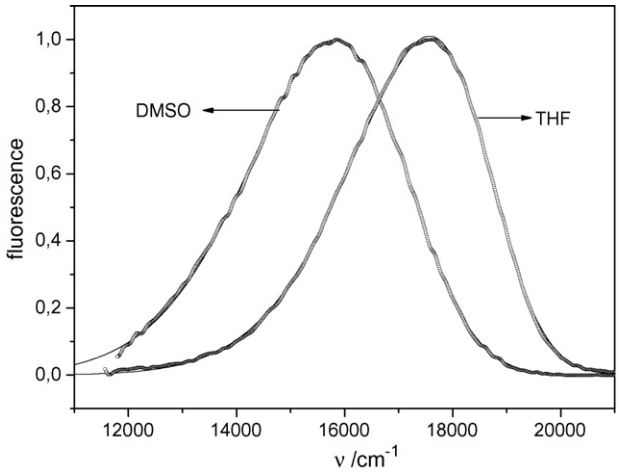

Fig. 7. Corrected and normalized CT fluorescence spectra of PQ3 in THF and DMSO and their theoretical predictions given by Eq. (2). The fitted parameters are $\Delta G_{et} = -2.46$ (-2.404) eV, $\lambda_s = 0.257$ (0.343) eV and $\lambda_{in} = 0.13$ eV for both solvents. The values in parentheses correspond to DMSO solution.

was obtained from the semiempirical calculations and gave the value 4.19*D* whereas the Lippert–Mataga analysis provided the value of $\Delta\vec{\mu}$ equal to 11.9 (1.1)*D*. For parent molecule PQ1, according to the HYPERCHEM calculations the ground state dipole moment is equal 2*D*. The semiempirical results are further confirmed by a more sophisticated method (DFT, B3LYP hybrid functional, 6-31+g* basis set), which produced the value for the ground-state dipole moment to be 2.40 and 4.42*D* for PQ1 and PQ2, respectively. This allows one to consider the semiempirical values for all the molecules as somewhat more credible; at least as far as the ground state dipole moments are concerned. We conclude that for the compounds that have the electrodonating group ($N(CH_3)_2$) and the electroaccepting group (CN) introduced into the parent molecule the emitting singlet state has a strong charge transfer character with the excited state dipole moments reaching 20.4 and 21.4*D* for PQ3 and PQ4, respectively. The fluorescence of these compounds can therefore be analysed in terms of the Marcus' radiative back electron transfer theory [19]. The CT fluorescence profile is described by the following formula [20] as

$$\mathrm{CT}(\nu) = n^3\nu^3\left(\frac{n^2+2}{3}\right)^2\frac{64\pi^2}{3h^3}M^2\sum_{j=0}^{\infty}\frac{S^j}{j!}(4\pi\lambda_s kT)^{-1/2} \times \exp\left(-\frac{(\Delta G_{et} + jh\nu_v + \lambda_s + h\nu)^2}{4\lambda_s kT}\right), \quad (2)$$

where M is the transition dipole moment, λ_s the solvent reorganization energy, ΔG_{et} the energy difference between the CT and ground states, S the displacement parameter, connected with the internal reorganization energy (λ_{in}) and the energy of the ring skeletal vibration ($h\nu_v = 1600\,\mathrm{cm}^{-1}$) by the relation:

$$S = \frac{\lambda_{in}}{h\nu_v}. \quad (2a)$$

Minimization procedure applied for theses systems in solvents of different polarity shows that the internal reorganization energy parameter (λ_{in}) does not depend on the polarity of the solvents and achieves a common (mean) value equal to 0.13 eV.

The solvent reorganization energy, which describes the motions of the solvent molecules during the charge transfer process, may be calculated using the formula [21]:

$$\lambda_s = \frac{\Delta\vec{\mu}^2}{4\pi hc\varepsilon_0 a^3}\left(\frac{\varepsilon_s - 1}{2\varepsilon_s + 1} - \frac{n^2 - 1}{2n^2 + 1}\right). \quad (2b)$$

Eq. (2) describes experimental findings remarkably well, which can be seen in Fig. 7, which presents a fit of the calculated fluorescence profile to the experimental one for PQ3 measured in two solvents of different polarity.

As expected, the values of the solvent reorganization energy increase with increasing solvent polarity, which also causes the decrease of the energy gap between the charge transfer and ground states. Both behaviours are depicted in Figs. 8 and 9.

The solvent dependence of the energy gap between the charge transfer state and the ground state is described by the relationship [22]:

$$\Delta G_{CT} = \Delta G_{CT}\,(\mathrm{vacuum}) - \frac{\vec{\mu}_e^2 - \vec{\mu}_g^2}{4\pi\varepsilon_0 a^3}\left(\frac{\varepsilon_s - 1}{2\varepsilon_s + 1}\right), \quad (3)$$

where ΔG_{CT} (vacuum) is the energy gap between these states in vacuum. The other parameters have been introduced previously. The equation predicts that increasing solvent polarity causes a decrease of the energy gap between the excited charge transfer state and the ground state, which is indeed observed (cf. Fig. 8).

Solvent polarity influences also the external reorganization energy. The mathematical description of this dependency is given by Eq. (2b).

As expected, with increasing solvent polarity, defined by the solvent polarity function $f(\varepsilon_s, n^2) = (((\varepsilon_s - 1)/(2\varepsilon_s + 1)) - ((n^2 - 1)/(2n^2 + 1)))$, the external reorganization energy increases.

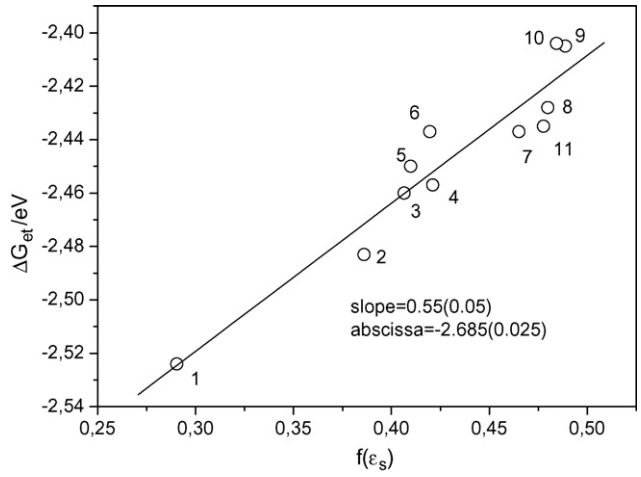

Fig. 8. Solvent polarity dependence of the free enthalpy change for the back electron transfer for compound PQ3. Solvent polarity function is given by $f(\varepsilon_s) = ((\varepsilon_s - 1)/(2\varepsilon_s + 1))$ (correlation coefficient $R = 0.96$). Indications of the solvents are given in the caption of Fig. 6.

Having the absorption spectra one can readily determine the molar extinction coefficients, and subsequently the absorption transition dipole moments, whereas the fluorescence quantum yields and lifetimes allow for calculation of the transition dipole moments for the emission. The absorption transition dipole moment is given by the formula [23]:

$$M_A^2 = 9.1853 \times 10^{-3} \frac{1}{n} \int \frac{\varepsilon(\nu)}{\nu} \, d\nu. \tag{4}$$

The integral in Eq. (4) denotes the integrated reduced molar absorption and the constant in Eqs. (4) and (5) emerges from simple calculations of the basic physical constants (Planck' and Avogadro's constants, velocity of light c, etc.).

The electronic transition dipole moment M_{fl} is defined as

$$k_f = \frac{\Phi_f}{\tau_f} = \frac{1}{3.1887 \times 10^6} (n\nu_{av})^3 M_f^2, \tag{5}$$

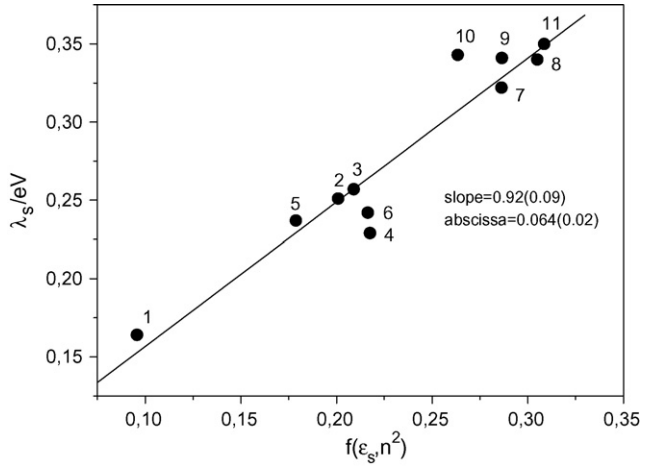

Fig. 9. Solvent polarity dependence of solvent reorganization energy for PQ3. Solvent polarity function is given by $f(\varepsilon_s, n^2) = (((\varepsilon_s - 1)/(2\varepsilon_s + 1)) - ((n^2 - 1)/(2n^2 + 1)))$ (correlation coefficient $R = 0.955$). Indications of the solvents are given in the caption of Fig. 6.

in which the averaged emission frequency is given by Ref. [14]:

$$\nu_{av} = \frac{\int I(\nu)\nu \, d\nu}{\int I(\nu) \, d\nu}. \tag{5a}$$

We can see in Table 1 that for each molecule under study the transition dipole moment for absorption and for emission are approximately the same (there only seems to be a small drop with increasing solvent polarity). This finding may be attributed to the lack of significant conformational changes between the ground and emissive singlet states [24].

What is far more striking is the fact that the transition dipole moment largely increases when the electron donating group ($N(CH_3)_2$) is introduced into the pyrazoloquinoline moiety.

3.2. Non-radiative back electron transfer transition

Transient absorption spectra of the investigated pyrazoloquinolines taken in the nanosecond time scale do not indicate a significant transient absorption in any solvents [25]. In low temperature measurements we found only traces of an additional band located around ca. 2.0 eV which may be attributed to the phosphorescence on the basis of comparison with the findings reported by Kucybala et al. [26].

We can conclude that the most important deactivation pathways of the emitting singlet state are fluorescence and radiationless transitions leading to the ground state recovery of the dyes.

As mentioned previously, the clear CT fluorescence has been observed for the systems containing electron donor and electron acceptor subunits (i.e. in PQ2, PQ3 and PQ4). From the basic fluorescence measurements we have calculated the rate constants of the non-radiative transitions that deactivate the emitting singlet state. The results are presented in Fig. 10.

The explanation of this fact is as follows. All the three compounds consist of the same electron donor unit; they differ only with respect to the presence of the *p*-cyano group at either of the phenyl rings attached to the pyrazoloquniline skeleton in the 1 or 3 position. This alters the energy gap between the emitting singlet excited state and the ground state. This plot provides a plateau at higher emission wavenumbers which may be attributed to the very small non-radiative rate constant (intersystem crossing). Decreasing energy gap between the charge transfer and the ground states causes an increase of the non-radiative rate constant as it emerges from the Marcus theory for the inverted region. A confirmation of the validity of our conclusion may be achieved by simple calculation of the non-radiative back electron transfer rate constants using the electron transfer parameters obtained from the charge transfer fluorescence band analysis.

However, to complete the parameters which are necessary to calculate the back electron transfer rate constants we need to estimate the electronic coupling matrix element, V. To do that we make use of the following equation [21,22]:

$$M_{fl} = V_0 \frac{\Delta\mu}{hc\nu_{CT}} + \sum_i \frac{V_i M_i}{E_i - hc\nu_{CT}} \tag{6}$$

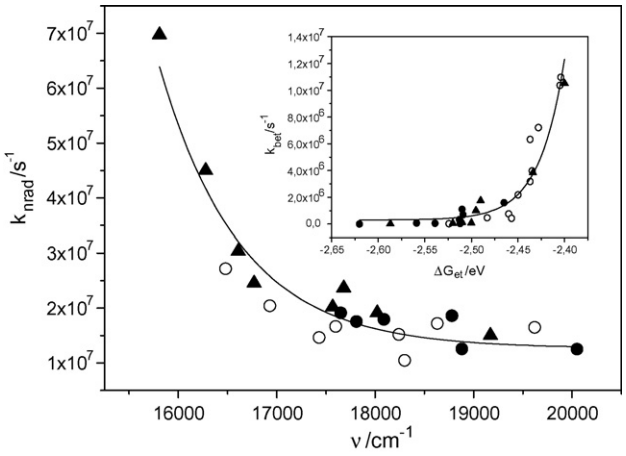

Fig. 10. Dependence of non-radiative rate constant on maximum of fluorescence emission for the investigated pyrazoloquinolines, PQ2: black circles; PQ3: black triangles and PQ4: open circles. The non-radiative rate constants were calculated from the relation, $k_{\mathrm{nrad}} = (1 - \Phi_{\mathrm{f}})/\tau_{\mathrm{f}}$. The correlation line is drawn only for presentation purpose. Inset-calculated non-radiative back electron rate constant versus ΔG_{et} for substituted pyrazoloquinolines. The parameters used in calculations were obtained from the CT fluorescence band shape analysis, the electronic coupling matrix element $V_0 = 0.27$ eV, the internal reorganization energy $\lambda_{\mathrm{i}} = 0.18$ eV, and energy of high-frequency internal vibration $h\Omega = 0.15$ eV.

where V_0 and V_i are the electronic coupling matrix elements between the CT and the ground states, and between the CT state and the ^{1}LE states of the energy E_i, respectively and M_i is the electronic transition moment between the ^{1}LE state of energy E_i and the ground state. We found that for the studied series of substituted pyrazoloquinolines (compounds PQ2–PQ4) the first term in Eq. (6) is most important at least in solvents of medium and high polarities. The calculated (mean) value of the parameter V_0 is equal to 0.27 (±0.2) eV. A small enhancement of the transition moment when solvent polarity decreases may be explained by increasing importance of the second term in Eq. (6) due to smaller energy gap between the charge transfer state and the locally excited singlet states.

For a non-adiabatic electron transfer process[1] the following formula for the rate constant holds [27]:

$$k_{\mathrm{et}} = \sum_{j=0}^{\infty} \frac{2\pi V_0^2 \exp(-S) S^j / j!}{h(4\pi\lambda_{\mathrm{s}} kT)^{1/2}} \exp\left(-\frac{(\Delta G + jh\Omega + \lambda_{\mathrm{s}})^2}{4\lambda_{\mathrm{s}} kT}\right). \quad (7)$$

The parameters appeared in this equation have been defined previously. It should be noted that important parameters such as λ_{s}, ΔG_{et} and λ_{in} have been estimated from the CT fluorescence band shape analysis (Eq. (2)). The theory predicts an increase of the back electron transfer rate constant when the energy gap between the CT and the ground states decreases (the free enthalpy parameter ΔG_{et} becomes more positive) as it is presented in the inset for Fig. 10 as the dependence of the non-radiative rate constant as a function of the position of the CT fluorescence maximum. This dependence is true because there is a simple linear relationship between the free enthalpy change (ΔG_{et}) and the position of the maximum of the CT fluorescence [21,22,24]:

$$\tfrac{1}{2}(hc\nu_{\mathrm{abs}} + hc\nu_{\mathrm{fl}}) \cong -\Delta G_{\mathrm{et}}, \quad (8)$$

where $hc\nu_{\mathrm{abs}}$ and $hc\nu_{\mathrm{fl}}$ is the position of the absorption and emission maximum, respectively. Due to weak solvent dependence of the position of the 0–0 absorption band the free enthalpy change is a linear function of the position of the fluorescence maximum. Thus the increase of the measured back electron transfer rate constant with decreasing values of the maximum of the CT fluorescence is explained.

4. Conclusions

Derivatives of pyrazoloquinolines show a single-band fluorescence emission at room temperature, which in three cases reveals a pronounced charge transfer character of the emitting singlet state. This is proven, e.g. by the solvatochromic shift of the position of the fluorescence maximum. The charge transfer fluorescence analysis on the basis of the Marcus theory for the radiative electron transfer transition yields the values of the charge transfer parameters such as the free enthalpy change and the external reorganization energy, which show significant changes when the solvent polarity is altered. The internal reorganization energy seems to be solvent independent. The transition dipole moments calculated from the absorption spectra (M_{a}) and the fluorescence characteristics (M_{fl}) show only a small variation with changing solvent polarity. For the studied compounds PQ2–PQ4 they are almost identical.

Acknowledgements

This work was supported by the State Committee of Scientific Research of Poland (Grants Nos. 3 T09A 102 18 and 4 T09A 109 25). We would like to thank Prof. Jan Najbar for diverse help in the course of completion of this project and Dr. Andrzej M. Turek for editorial comments.

References

[1] A. Musierowicz, S. Niementowski, Z. Tomasik, Rocz. Chem. 8 (1928) 325.
[2] R.R. Crenshaw, G.M. Luke, P. Smirnoff, J. Med. Chem. 19 (1976) 262.
[3] P. Smirnoff, R.R. Crenshaw, Antimicrob. Agents Chemother. 11 (1977) 571.
[4] R.G. Stein, H.J. Biel, T. Singh, J. Med. Chem. 13 (1970) 153.
[5] A. Brack, Liebig Ann. Chem. 681 (1965) 105.
[6] K. Rechthaler, K. Rotkiewicz, A. Danel, P. Tomasik, K. Khatcharian, G. Kohler, J. Fluoresc. 7 (1997) 301.
[7] K. Rurack, A. Danel, K. Rotkiewicz, D. Grabka, M. Spieles, W. Rettig, Organic Lett. 4 (2002) 4647.
[8] J.-H. Pan, Y.-M. Chou, H.-L. Chiu, B.-C. Wang, Tamkang J. Sci. Eng. 8 (2005) 175.

[1] A relatively large electronic coupling matrix element V_0 indicates that the electron transfer is an adiabatic process with the rate constant depending on the so-called longitudinal relaxation time of the solvent. However, for the back electron transfer in the inverted Marcus region the rate constants calculated from the Jortner formula gave the same results as calculated from the Onuchic equation for the adiabatic electron transfer rate constant.

[9] Z. He, G.H.W. Milburn, A. Danel, A. Puchała, P. Tomasik, D. Rasała, J. Mater. Chem. 7 (1997) 2323.
[10] K. Araki, J. Funaki, A. Danel, P. Tomasik, Polish J. Chem. 78 (2004) 843.
[11] A. Danel, Z. He, G.H.W. Milburn, P. Tomasik, J. Mater. Chem. 9 (1999) 339;
M. Rymarczyk-Machal, S. Zapotoczny, M. Nowakowska, J. Polym. Sci. A Polym. Chem. 44 (2006) 2675.
[12] K. Ozga, E. Gondek, A. Danel, K. Chaczatrian, Opt. Commun. 231 (2004) 437.
[13] A.B.J. Parusel, R. Schamschule, G. Köhler, J. Mol. Struct. (Theochem.) 544 (2001) 253.
[14] M. Mac, A. Danel, A. Wisła, A. Karocki, R. Królicki, J. Photochem. Photobiol., Chem. A 180 (2006) 88.
[15] P. Tomasik, D. Tomasik, R. Abramovitch, J. Heter. Chem. 20 (1983) 1539.
[16] S.R. Meech, D. Phillips, J. Photochem. 23 (1983) 193.
[17] M. Mac, A. Danel, K. Kizior, P. Nowak, A. Karocki, B. Tokarczyk, Phys. Chem. Chem. Phys. 5 (2003) 988.
[18] E. Lippert, Z. Naturforsch. 10a (1955) 541;
N. Mataga, Y. Kaifu, M. Koizumi, Bull. Chem. Soc. Jpn. 28 (1955) 690.
[19] R.A. Marcus, J. Phys. Chem. 93 (1989) 3078.
[20] I.R. Gould, R.H. Young, L.J. Mueller, A.C. Albrecht, S. Farid, J. Am. Chem. Soc. 116 (1994) 8188;
I.R. Gould, R.H. Young, R.E. Moody, S. Farid, J. Phys. Chem. 95 (1991) 2068.
[21] J. Herbich, A. Kapturkiewicz, Chem. Phys. 170 (1993) 221.
[22] P. Borowicz, J. Herbich, A. Kapturkiewicz, M. Opallo, J. Nowacki, Chem. Phys. 249 (1999) 49.
[23] J.E. Lewis, M. Maroncelli, Chem. Phys. Lett. 282 (1998) 197.
[24] A. Kapturkiewicz, J. Nowacki, J. Phys. Chem. A. 103 (1999) 8145.
[25] M. Mac, T. Uchacz, M. Andrzejak, A. Danel, P. Szlachcic, Photophysical properties of pyrazoloquinolines and pyrazoloquinoxalines, in preparation.
[26] Z. Kucybala, A. Kosobucka, J. Paczkowski, J. Photochem. Photobiol. Chem. A 136 (2000) 227.
[27] J. Jortner, J. Chem. Phys. 64 (1976) 4860.